Journal of Environmental Geography 16 (1–4), 1–10.

DOI: 10.14232/jengeo-2023-44452
ISSN 2060-467X

COMPARATIVE EVALUATION OF THE MATERIAL OF THE ARTIFICIAL LEVEES: A CASE STUDY ALONG THE TISZA AND MAROS RIVERS, HUNGARY

Diaa Sheishah[1,2], György Sipos[1*], Károly Barta[1], Enas Abdelsamei[1,2], Alexandru Hegyi[3], Alexandru Onaca[3], Abbas M. Abbas[2]

[1]University of Szeged, Department of Geoinformatics, Physical and Environmental Geography, 6722 Szeged, Egyetem u. 2-6., Hungary
[2]National Research Institute of Astronomy and Geophysics, 11421, El Marsad st., Helwan, Cairo, Egypt
[3]Applied Geomorphology and Interdisciplinary Research Centre (CGACI), Department of Geography, West University of Timisoara, 300223 Timisoara, Romania
*Corresponding author, email: gysipos@geo.u-szeged.hu

Research article, received 1 February 2023, accepted 22 February 2023

Abstract

Artificial levees have major importance in protecting human lives and infrastructure as they are essential elements of the flood protection measures. Nevertheless, the lack of the necessary information about their structure and internal composition might cause high risks. To monitor their stability, integrated surveys are needed, including geophysical and geotechnical methods. Levees along the rivers in Hungary were constructed more than 150 years ago, and they were heightened several times; therefore, investigations are required to assure their performance in flood risk mitigation. Our investigation aimed to utilise non-invasive geophysical techniques, primarily electrical resistivity imaging, with the validation of geotechnical investigations to map and compare the compositional and structural variations of two very different levee sections along River Tisza and River Maros. Integrating the analysed drilling data with ERT profiles showed that the main composition of the investigated Tisza levee section is fine and medium silt with an average resistivity 30 Ωm, however, the investigated section of Maros levee was built of not only of fine and medium silt but also of medium and coarse sand exhibiting higher resistivity values reaching up to 2200 Ωm. Several physical parameters were measured to study the nature of constituting levee materials like moisture content, grain-size, porosity, bulk-density, saturated hydraulic conductivity, and resistivity. It was found that most of them show a connection with resistivity, but the hydraulic conductivity did not show a direct connection, however the latter could exhibit the aquitard nature of Tisza levee materials and the non-aquitard nature of Maros levee materials.

Keywords: artificial levee composition, alluvial rivers, Electrical Resistivity Tomography (ERT), flood risk, drillings

INTRODUCTION

The artificial levee is essentially a barrier constructed parallel to river channels to prevent flooding during high discharge stages (Alexander et al., 2012). Flood protection in Hungary depends primarily on artificial levees: their total length is around 4200 km in the country. The Tisza River and its tributaries have a 65% share of this value, making the river system, in this respect, one of the most heavily engineered rivers on Earth (Nagy, 2010). The levee systems along the rivers in Hungary were built 150 years ago, and their structure and internal composition are hardly known. Along most of the rivers in Hungary, the first artificial levees were not high enough, and periodic floods overtopped them frequently. Therefore, their size and height were continuously increased, especially after high and strong flood events. This resulted in the evolution of complicated earth structures with spatially variable composition (Galli, 1976; Schweitzer, 2002). Furthermore, levees were then affected by various post-constructional processes, such as subsidence, compaction and water seepage during floods (Galli, 1976; Kovács, 1979; Tímár, 2006).

Artificial levees in Hungary were constructed of compacted sediments. The least permeable sediments, such as clays were placed at the riverside of the levee. The heights of the levees are variable and are designed based on various factors, such as the estimated highest flood stage, material type, types of land use and structures behind the levee, foundation, and the availability of land for construction (Lászlóffy, 1982; Kiss et al., 2019).

Flood risk related to levee failure has become an important investigation issue in many countries because of the climate change which sometimes leads to extreme flood events and hence the related hazards. The interest in applying advanced techniques that can efficiently evaluate the internal composition of artificial levees has become one of the decision-maker priorities, especially the geophysical techniques that have been progressively implemented by many authors to flood risk mitigation (Asch et al., 2008; Di Prinzio et al., 2010; Hibert et al., 2012; Morelli and Francese, 2013; Chlaib et al., 2014; Busato et al., 2016; Borgatti et al., 2017; Bakula et al., 2017; Crawford and Bryson, 2018). Since their construction, several issues may decrease the resistance of levees and hence increase flood risk. Water can pass through the levee body and weaken the structure internally at the interface between layers and in layers with coarser grain sizes (Casagrande, 1937; USACE, 2000). The process can be accelerated by cracks and animal burrows (Nagy, 2010). Seepage can also occur below the levee in higher porosity sediments, resulting in the development of sand boils (Li et al., 1996), which can easily lead to the failure of the structure (Desai, 1970; Ojha et al., 2001). Bearing in mind the above issues and the ageing of levees, it is ultimately important to map and survey their structure, composition and condition to prevent hazardous situations.

The utilisation of electrical resistivity imaging became state-of-the-art in studying levees (Cho and Yeom, 2007; Sjödahl et al., 2009; Sheishah et al., 2022), together with ground-penetrating radar (Di Prinzio et al., 2010). Integrating two or more different geophysical techniques can provide more reliable results (e.g. Inazaki and Sakamoto, 2005; Cardarelli et al., 2014). However, best interpretations can be made by validating them using geotechnical inspection (e.g. Perri et al., 2014).

Electrical resistivity values depend on many physical parameters such as porosity, bulk-density, grain-size, and degree of water saturation (Loke 2004; Samouelian et al., 2005; Jerabek et al., 2017; Romero-Ruiz et al., 2018;). Increased bulk density and reduced porosity are considered as the main parameters increasing the compaction of the soil. Therefore, it is expected that compacted soils have lower electrical resistivity values (Zhu et al., 2007). From this aspect, ERT is a promising technique in recognising the structure differences because of soil compaction (García-Tomillo et al., 2018) It also provides more information about the spatial variations in both the horizontal and vertical direction (Robinson et al., 2008). Therefore, the main objectives of the current research are (1) to determine and compare the structure and composition and resistivity range of two different levee sections along the Tisza and Maros Rivers, using ERT and borehole data; (2) to identify the relationships between the specific resistivity values and different geotechnical parameters, such as grain size, saturated hydraulic conductivity (k), density, porosity and moisture content; and (3) to classify the main levee components regarding hydraulic conductivity, and attributing typical resistivity values to them.

DATA AND METHODS

Study Area

The Tisza River is the largest tributary of the Danube: its length is 962 km, the area of its catchment is 157 000 km^2, while its mean discharge at Szeged, close to the study site and not far from its confluence with the Danube, is 865 m3/s. Before the great-scale regulation works of the 19th century, the lowland section of the river was characterised by extensive floodplains (38 500 km^2) inundated almost every year, thus making agricultural activity difficult (Kovács, 1979). The Maros is one of the major rivers originating in the Transylvanian Basin, Romania. It reaches the Great Hungarian Plain along the southern periphery of the Körös Depression. The Maros became the main river of the Basin, when the Gheorgheni Basin, situated between the Eastern Carpathians and the interior volcanic belt, was dewatered partly by back cutting and partly by antecedence during the Eopleistocene. The river occupied its present position at the end of the Pleistocene, due to tectonic movements.

To create flood-safe areas, artificial levees in Hungary were built, especially in the second half of the 19th century, which confined the floodplain width to 0.4–5 km (Kiss et al., 2021). The width of the active confined floodplain is irregular, therefore the flood hazard is increased in the narrowing sections (Lóczy et al., 2009). These linear man-made earthworks were built along rivers, to inhibit the inundation of distal floodplain areas (Szűcs et al. 2019, Knox et al. 2022). The main source of the material of artificial levees in Hungary was the nearby floodplain sediments. Clay is the main component of their core, covered by compacted fine-grained sediments like silt. At some levee parts, the protected side is covered by sandy layers to help in the draining of the levee core during floods (Szűcs et al., 2019). Since their construction, levees have been heightened gradually as flood levels increased continuously (Lóczy et al., 2009) resulting in very complex earthen structures with several layers (Kovács, 1979; Nagy, 2010). Their current height is 5–7 m. The height of the artificial levees in the area was increased after the record flood of 1970 to provide flood safety. In the meantime, because of their high age, limited information on their condition and its change through time is known.

The study was made at two sites: the first is located on the left bank of Tisza River, and the second is located on the left bank of its tributary, the Maros River (Fig. 1). The centre point of the first site is at 31.4 Lkm (Lkm stands for levee kilometre, which is measured either from the confluence or the country's national border) and the centre point of the second zone is at 3 Lkm. The relative height of the levee at the first site is ~ 6.5 m, while at the second it is ~ 5 m. The investigated levees were last reinforced in the early 1970s, but little is known about their internal structure and the composition of their layers.

Geophysical data acquisition and processing

Electrical Resistivity Tomography (ERT) was selected among the other geophysical techniques to conduct the current survey because of its high potentiality in detecting compositional differences and anomalies at greater depths, though at limited resolution. ERT data were collected using a GeoTom MK8E100 apparatus connected to a multi-electrode system (25 electrodes) (Fig. 2A and B). A total of four ERT profiles were collected: one longitudinal and one transverse profile on the Tisza levee (Fig. 1C). Another two profiles were collected in the same way on the Maros levee; (Fig. 1D). The Wenner array was used for data collection since, regarding most common measurement arrays, it has the strongest signal strength and is relatively sensitive to vertical changes in subsurface resistivity values below the centre of the array (Loke, 2004). The two longitudinal profiles were measured using 2.5 m electrode spacing. The transverse profiles, perpendicular to the previous two, were collected using a 2 m electrode spacing. The number of depth levels was set to 8 in each case, and consequently, 92 data points were acquired per profile. Regarding the

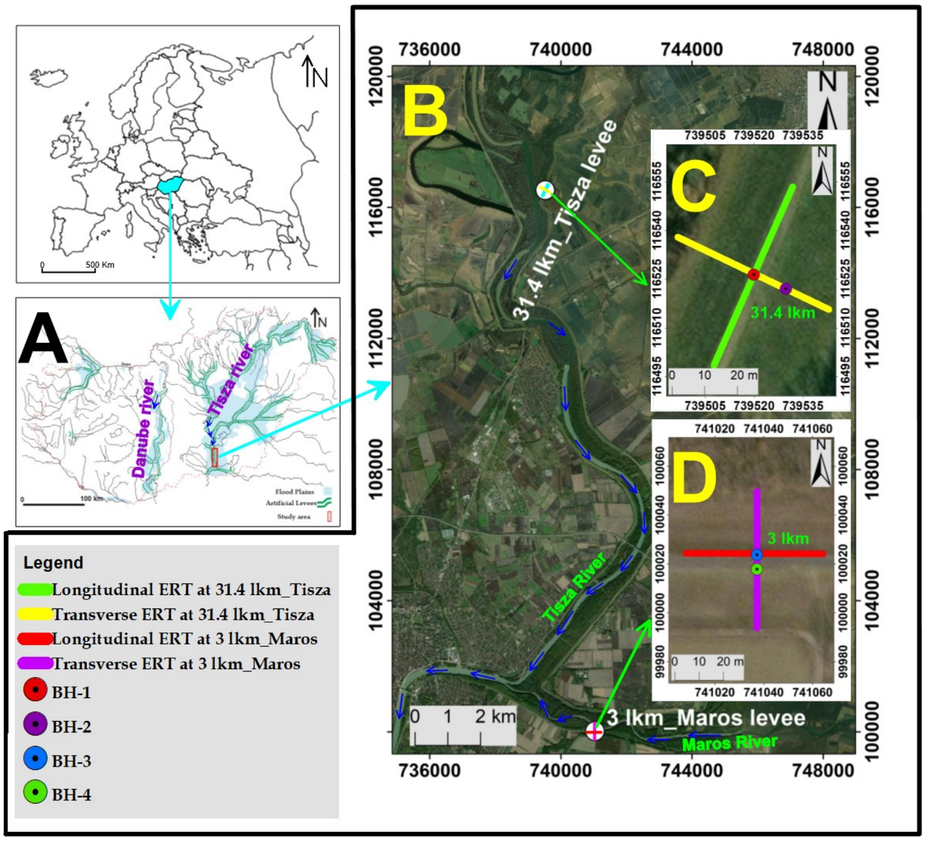

Fig. 1 Location of the study area and the survey plan.
A) Artificial levees and potential floodplains along rivers in Hungary (modified after OVF 2014). B) Location of the ERT measurement sites on the Tisza and Maros levees. C) Location of ERT profiles and boreholes on Tisza levee. D) Location of ERT profiles and boreholes on Maros levee.

transverse profiles, elevation data were measured by a TopCon Hyper Pro RTK GPS at each odd electrode along the surveyed line to apply a topographic correction for the ERT profiles.

In order to obtain the true resistivity values for different levee materials, apparent resistivity obtained by ERT profiling was processed with software RES2DINV 3.4 (Loke, 2004). Before initiating the inversion process, noisy outlying data points were taken out. The inversion scheme was based on the least-squares smoothness constrained iterative optimisation algorithm (Constable et al., 1987; De Groot-Hedlin & Constable, 1990). Because the transverse profiles show elevation changes depending on the levee shapes, a topographic adjustment was also carried out before initiating the inversion. After obtaining satisfactory RMS values, the inverted ERT profiles were exported and drawn in Surfer v14 for evaluation with the help of borehole information.

Geotechnical data analysis

In order to precisely interpret ERT profiles, in total, four boreholes were drilled. Two boreholes were drilled on the Tisza levee at 31.4 Lkm, one on the riverside edge of the levee crown (BH-1) and another on the protected side slope of the levee (BH-2) (Fig. 1C). The other two boreholes were drilled on the levee of the Maros at 3.0 Lkm at similar positions (BH-3 on the crown, BH-4 on the protected side slope) (Fig. 1D). The drillings were made in the ERT survey lines right after geophysical data acquisition. Drilling depths for boreholes BH-1, BH-2, BH-3, and BH-4 were 6 m, 4 m, 7 m and 2.8 m, respectively. An Eijkelkamp corer with a 5 cm diameter drilling head was used (Fig. 2C). Topcon Hyper Pro RTK GPS was also used to record the exact position and elevation of drilling locations to correctly locate them on ERT profiles.

Simultaneously, samples were collected at every 20 cm for grain-size analysis, which was performed with a Fritsch Analysette 22 laser diffraction analyser, having a measurement range of 0.08-2000 µm. Samples underwent ultrasonic homogenisation, and all measurements were repeated three times to check if there was further disintegration (Kun et al. 2013). Sample D50 values were applied for controlling geophysical results, and the mean grain-size fraction of samples was classified using the Udden-Wentworth scale.

Besides, samples were also taken for water content analysis at every 40 cm. Samples were dried at 100°C in an oven overnight. Percentage gravimetric water content was determined by subtracting sample dry weight from wet weight and dividing the product with dry weight.

The saturated hydraulic conductivity of levee material is very important from the aspect of flood water retention. In order to assess this parameter, thus 13 samples were collected in undisturbed soil sample cylinders during the drilling procedure. The samples were taken where compositional changes were identified. Five samples were collected from BH-1 at depths of 1.5 m, A B C

Fig. 2 Data acquisition by GEOTOM MK8E100 multi-electrode ERT system at 31.4 Lkm of Tisza levee (A), and 4 Lkm of Maros levee (B). Drilling boreholes by using an Eijkelkamp drilling system (C).

1.6 m, 2.5 m, 4.1 m, and 4.2 m. Five samples were collected from BH-3 at depths 1.5 m, 1.6 m, 2.9 m, 6.1 m, and 6.2 m. Three samples were collected from BH-4 at depths of 1.5 m, 1.6, and 2.85 m. No significant changes in composition were noticed in terms of borehole BH-2.

The bulk density was obtained from the weight of the dry samples divided by the volume of the soil sampling cylinder. The total porosity was calculated as

$$n=100\ [1-\rho_b\rho_d] \quad (1)$$

where

n: the total porosity (%);
ρ_b: the bulk density of the material (g/cm^3);
ρ_d: the particle density of the material (g/cm^3).
Particle density was considered to be 2.65 g/cm^3 (Fetter, 2001).

Saturated hydraulic conductivity was determined on the basis of the Darcy's law, i.e. the flow through a medium directly proportional to the height of the hydraulic head and inversely proportional to the length of the flow path. Flow was also determined by coefficient K, which depends upon the porous medium's nature. The value of K was determined by an infiltrometer, using the falling-head method for fine grained samples like fine and medium silt and constant head method for coarse grained samples like sand (Dane and Hopmans, 2002; Reynolds and Elrick, 2002). Following the measurements, samples were dried at 100°C, and their weight was measured using a precision scale to calculate bulk density. Based on density values, porosity was also determined by taking the standard particle density of soils.

RESULTS

Geophysical results

The difference in the composition of Tisza and Maros levees is clearly visible in the resistivity results. In general, the inverted ERT profiles exhibited low resistivity values in the case of Tisza levee and medium and high values in the case of Maros levee. The longitudinal and transverse profiles measured on the Tisza levee exhibited a range of values from 6 Ωm to 60 Ωm with an average of 17 Ωm. In the case of the longitudinal profile measured on the Maros levee, values ranged between 15 Ωm and 46 Ωm with an average of 30 Ωm. In the Transverse profile measured on the Maros levee, values were considerably higher, reaching a maximum of 2200 Ωm and the mean specific resistivity was 660 Ωm (Fig. 3).

The combination of sedimentological information and ERT profiles also referred to the layered structure of the body of both levee sections. The electrode spacing is an important factor in the resolution of ERT data. The 2 m electrode spacing can provide 1 m vertical resolution, which could resolve the levee layers in this range or above. The maximum survey depth of the profiles at this resolution was between 8 and 13 m, which is more than the relative height of the levee; therefore, the layers below the levee could also be investigated.

The longitudinal profile measured at the investigated site of the Tisza levee exhibited two units; the first unit is the dominant component of the levee body, with resistivity value ranging between 6 Ωm and 20 Ωm until a depth of 5.5 m. Then the second unit was noticed below this depth with resistivity value ranging between 21 Ωm and 60 Ωm (Fig. 3A). The transverse profile measured at this zone exhibited the same unit succession with approximately the same resistivity range. In addition, a third unit was noticed at the top 1 to 2 m of both sides of the Tisza levee with resistivity values ranging between 16-61 Ωm (Fig. 3B).

The materials forming the Maros levee differ from that found in the Tisza levee. Three successive units were identified in the longitudinal ERT profile measured on the crown of the Maros levee, at 0–0.8 m, 1–4.4 m, and 4.6–7 m with resistivity values ranging between 15–26 Ωm, 31–46 Ωm, and 15–30 Ωm respectively (Fig. 3C). The variation in Maros levee composition could be even more visible, especially on the protected side. Three units could be resolved; the first unit (thickness ~ 0.6 m) has a resistivity range between 5 and 270 Ωm, the second unit (thickness ~ 1.6 m) has a resistivity range between 270 and 1636 Ωm, the third unit (thickness ~ 1.6 m) is in the form of a lense of very high resistivity and has a range between 1700 and 2200 Ωm (Fig. 3D). To see the interface that separates two fine grained units (fine and medium silts) in the riverside, a small scale 5–60 Ωm was applied on the transverse ERT profile measured on Maros levee section and the low resistivity range could help in separating the two compositions as shown in (Fig. 3E)

Geotechnical results

A) Analysis of borehole samples

The first borehole (BH-1) exhibited three units (Fig. 3E); a fine silty layer from the surface until a 0.4 m depth with a D50 value ranging between 9 and 11 µm, a medium silty layer at depths between 0.6–0.8 m with a D50 value ranging from 16 to 19 µm, and a fine silty layer again, below 1 m with a D50 value ranging from 9 to 14 µm (Table 1). The three individual units expose an overall mean grain size of 10 µm, 17 µm and 11 µm, respectively, meaning that even though there is some difference in grain size averages, the levee body is within the fine and medium silt range in general.

The second borehole (BH-2) exposed three units as well (Fig. 3F); a fine silty layer from the surface until a 1.4 m depth with a D50 value ranging from 10 to 15 µm, a thin layer of medium silt at depths between 1.6 and 1.8 m with a D50 value ranging between 23 and 24 µm, and a fine silty layer again, below 2 m with a D50 value ranging from 8 to 11 µm. The three individual units expose an overall mean grain size of 13 µm, 23 µm and 10 µm, respectively. This indicates that the protected side of the levee is composed of fine-grained sediments within the fine and medium silt range.

The third borehole (BH-3), drilled on the crown of the Maros levee, exposed three units (Fig. 3G). The first unit contained a fine silty layer (0–0.8 m) with a D50 value ranging between 12 and 14 µm, a thick layer of medium silt (1–4.4 m) with a D50 value ranging from 16 to 24 µm and a fine silty layer again below 4.4 m with a D50 value ranging between 12 and 15 µm. Unit means grain sizes were 13, 24 and 14 µm, respectively. It was noticed from the second and third units that the grain-size curve reflects sudden changes at some points, but these are not that significant to move the D50 value into another grain-size class. Consequently, we did not separate further sedimentary units at BH-3. The overall evaluation from BH-3 indicates that the Maros levee body is predominantly composed of fine-grained sediments.

The fourth borehole (BH-4) drilled on the protected side of the Maros levee exhibited five units (Fig. 3H); a fine silty layer from the surface until a 0.2 m depth with a D50 value of 15 µm, a medium silty layer at depths between 0.2–0.4 m with a D50 value 16 µm, a very fine sandy layer with a D50 value 104 µm, a thick medium sandy layer at depths between 0.6–2.2 m with a D50 value ranging from 292 to 453 µm with a mean grain size value 358 µm and a fine silty layer below 2.2 m with a D50 value ranging between 12 and 13 µm. The five units exhibit an increasing grain-size trend with depth, meaning that the coarse-grained sediments as sandy materials are the main components of the protected side of the Maros levee.

B) Analysis of saturated hydraulic conductivity

The average water content percentage for the five samples collected from the Tisza levee was similar to the average water content percentage for the eight samples collected from the Maros levee which was approximately 20%, therefore from the other parameters affecting resistivity, the resistivity range of the ERT profile measured transversely on Tisza levee is lower than that noticed by ERT profile measured transversely on Maros levee so, there is an indication that the materials forming the investigated Tisza levee are more compacted than the investigated Maros levee.

It was found that in the case of the five samples collected from the BH-1of Tisza levee, the grain-size range was from 10.8 to 13 µm with an average of 12 µm, the porosity percentage range was from 36 to 44 m/m% with an average of 40 m/m%, and bulk density range was from 1.50 to 1.69 g/cm^3 with an average of 1.6 g/cm^3. However, in the case of the eight samples collected from BH-3 and BH-4 of Maros levee, the grain size range was from 11.7 to 339.3 µm with an average of 142 µm. The porosity percentage range was from 41 to 47 m/m% with an average of 45.9 m/m%, and the bulk density range was from 1.32 to 1.56 g/cm^3 with an average of 1.44 g/cm^3.

Regarding the hydraulic conductivity analysis of 13 samples, the levee materials were classified as aquitard and non-aquitard. It was found that all the samples collected from the Tisza levee (5 samples) are aquitard because aquitard materials are a poorly permeable underground layer that limits the flow of water from the riverside to the protected side. This layer is important in the levee composition from the aspect of flood risk mitigation. In contrast, the samples collected from Maros levee (8 samples) are non-aquitard, except one sample at a depth of 290 cm collected on the levee crown aquitard. The samples taken from five different depths from BH-1 show similar low saturated hydraulic conductivity (0.013075 mm/h on average) because of the silty units forming the Tisza levee. At the same time, the situation in BH-3 and BH-4 is totally different. Regarding BH-3 drilled on the crown of Maros levee. The saturated hydraulic conductivity at the core of Maros levee at ~3 m depth is 0.0132 mm/h and shows similarity to that obtained by the Tisza levee; however, it is lower than that in the upper part of Maros levee ~1.5 m to 1.6 m (2.2222 mm/h on average) and the lower part of Maros levee ~6 m (0.4924 mm/h). In the case of BH-4

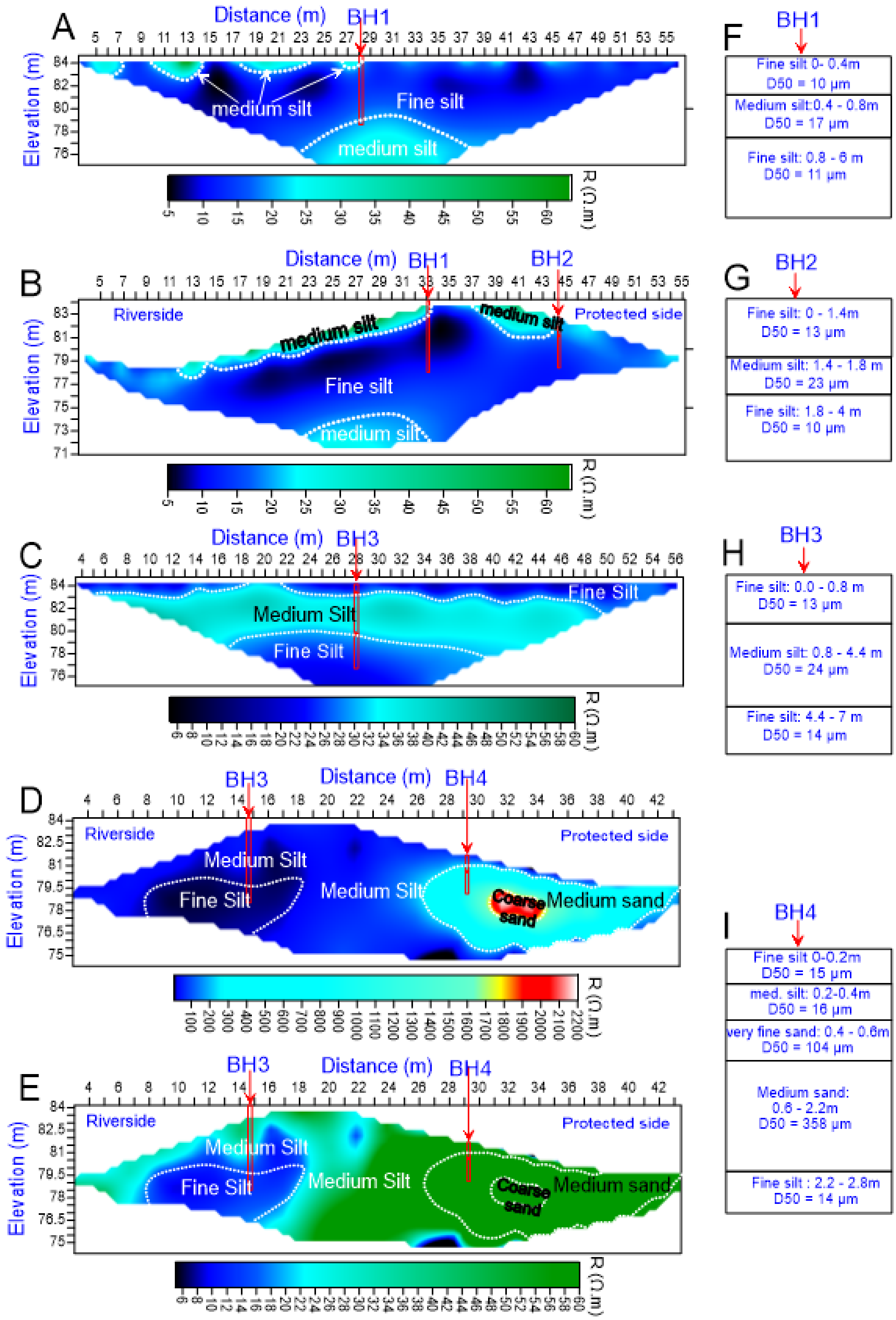

Fig. 3 Longitudinal (A) and transversal (B) electrical resistivity tomography profiles acquired on the Tisza levee at 31.4 Lkm. Longitudinal (C) and transversal (D) electrical resistivity tomography profiles acquired on the Maros levee at 3 Lkm. The same profile as the proceeding one (D) but with applying a small resistivity range between 5 and 60 Ω.m (E). Thickness and mean grainsize values of structural units, identified by drillings (F-I).

drilled on the protected slope of Maros levee, the saturated hydraulic conductivity recorded very high values at the levee top ~1.5 m to 1.6 m (406 mm/h on average) because of the sandy layer covering the protected side and very low value at the core of the levee ~2.8 m (0.0524 mm/h) because of the fine silty nature of the core.

DISCUSSION

The previous results, in general, could help to understand the structure of the two levee sections investigated. The contrast in the resistivity values of the investigated levee materials was clearly visible; therefore, the interfaces between layers could be detected using ERT, as it was documented earlier by other authors (e.g. Kearey et al., 2013; Sheishah et al., 2022).

ERT results, confirmed by sedimentological data showed that the core of the two investigated levee sections was different in the sense that the levee along the Tisza is composed of fine silt, while the levee along the Maros of medium silt. From the aspect of flood safety, the dominance of fine silt is advantageous, as it is highly aquitard based on hydraulic conductivity measurements. However, the presence of medium silt makes uncertainty in non-aquitard nature.

Regarding the structure of the Tisza levee almost the entire levee body is composed of fine silt, however below the levee body a medium silt zone can be identified, which can be an area of increased seepage during floods, being undesirable from the aspect of flood safety. Medium silt units were also identified on the river side, in the form of a 1 m thick blanket, and on the protected side as part of a reinforcement. On the protected side the application of less impervious materials are accepted to control seepage, however river side blankets are supposed to be composed of highly impervious materials to inhibit borrowing (USACE, 2000).

Regarding the levee section investigated along the Maros River the levee body is made up mainly of medium silt. A fine silt unit was identified on the riverside part of the levee, starting from a 1 m depth. This layer is important in increasing the imperviousness of the structure, however, it does not reach up to the surface of the levee, thus during high water levels the overlying medium silt layer can transfer water towards the protected side. However, the presence of a relatively thin fine silt blanket over the riverside and the crown of the levee can provide sufficient protection against the development of intensive seepage. It is important to note, that fine silt cover could not be detected on ERT profiles, and could only been resolved using drilling data.

Unlike the Tisza, the protected side of the Maros levee section is built up mostly of sand, covered by a thin fine and medium silt layer. High porosity, sandy layers on the protected side can ease the drainage of water from the levee body during floods, and can be advantageous from the aspect of flood protection. However, as the riverside structure also contains a non-aquitard medium silt layer, the rate of seepage can be very intensive and is only moderated by a thin fine silt layer on both sides. Based on the drillings a fine silt layer is situated below the sandy unit, though ERT measurements were unable to detect it due to the very high resistivity of coarse grained sand, which masks nearby lower values.

As it was shown previously by several authors physical properties of the sediment, such as grainsize, porosity and water content can greatly affect specific resistivity values (Popescu et al., 2016; Alpaslan and Bayram, 2020). In the case of the present study, by applying several data sources a range of specific resistivity values can be given for different sediments with variable water content.

Based on ERT measurements at dry conditions in the investigated Tisza levee section, the quartile function was utilized to calculate the specific resistivity range of different materials and the results showed that fine silt has a range between of 10 and 14 Ωm with an average of 12 Ωm and standard deviation 3.2. Medium silt has a range between 23 and 29 Ωm with an average of 26 Ωm and standard deviation 12. By the same way the resistivity range for the different materials of the investigated Maros levee section at higher water levels were: fine silt has a range between 19 and 27 Ωm with an average of 22 Ωm and standard deviation 5. Medium silt has a range between 36 and 39 Ωm with an average of 37 Ωm and standard deviation 13. In addition to that, medium sand forming representing the major composition of the protected side shows a range between 233 and 639 Ωm with an average of 320 Ωm and standard deviation 392 Ωm and the coarse sand exhibits a range between 1769 and 3075 Ωm with an average of 2240 Ωm and standard deviation 941 Ωm.

In general, the resistivity range of the fine grained sediments forming both the investigated levee sections can be specified: fine silt has a resistivity range between 10 and 27 Ωm, medium silt has a resistivity range between 23 and 39 Ωm.

The mentioned resistivity values of Tisza levee materials indicate that the levee is built up from fine-grain sediments as far as the low empirical values given for alluvial materials by former researches (Keller and Frischknecht 1966; Waxman et al., 1968; Abu-Hassanein et al., 1996; Giao et al., 2003; Loke 2004, Tabbagh et al., 2007; Sheishah et al., 2022). Also, the values of the levee body core are close to or even lower than those reported by Busato et al. (2016) who found that in an earthen levee composed mainly of clayey sand and having low moisture conditions, resistivity values ranged between 50–100 Ωm. Similarly, fine-grained materials in a dam structure had a specific resistivity below 100 Ωm (Himi et al. 2018; Jodry et al. 2019). Kalinski and Kelly (1993), Schwartz et al. (2008) and Gunn et al. (2015) proposed a relationship between resistivity and fine-grained sediments. Datsios et al. (2017) measured the electrical resistivity of sand, and it showed a value of 1350 Ωm or more in dry soil. This value can be matched with the resistivity of the sandy lense (with a resistivity up to 2200 Ωm) detected on the protected side of the Maros levee that represents one of its main components; however, it was not noticed in the analysed grain-size samples because BH-4 did not hit this lense.

In our study, the fine-grained materials forming the Tisza levee show a lower porosity and higher bulk density than the coarse-grained materials forming the Maros levee, in which the latter show a higher porosity percentage and a lower bulk density. As stated by Robain et al. (1996), Alakukku (1996) Richard et al. (2001) and Pereira et al. (2007), there is a link between electrical resistivity values and porosity as the soil compaction process increases bulk density, reduces the volume of large pores and, in turn, affects the physical properties of the soils. A normal relationship is proposed between resistivity and coarse-grained materials (Keller and Frischknecht, 1966). Therefore, it is realised that besides the compaction parameter mentioned above, the lower porosity is one of the essential factors behind the noticed lower resistivity values measured on Tisza levee section. In contrast to the Tisza levee section, the higher resistivity values of the Maros levee might be due to the higher porosity related to its coarse-grained composition. Sediments with higher water content normally show lower resistivity values (Loke, 2004). Soil compaction of the levee materials is mainly characterised by increased soil bulk density and reduced macroporosity. Therefore, compacted soils should have lower electrical resistivity values (Zhu et al., 2007). The dry density influences the resistivity of fine-grained soil (Beck et al., 2011). It is also a promising tool for identifying differences in structure due to soil compaction (Jerabek et al., 2017; García-Tomillo et al., 2018).

The spatial and temporal change in soil moisture content are challenging factors in determining saturated hydraulic conductivity (Farzamian et al., 2015). Otherwise, the saturated hydraulic conductivity measurements can be triggered with so-called pedotransfer functions, which estimate the infiltration rate with the help of easier measurable parameters. These parameters are particle size, bulk density, (effective) porosity, soil organic carbon, calcium carbonate and pH (Tóth et al., 2015; Ottoni et al., 2019). The complexity of the problem is clearly shown by the fact that there are dozens of pedotransfer functions, many of which have been applied in Europe as well (Nasta et al., 2021).

Pedotransfer functions are used to estimate the soil's electrical resistivity as well. Hadzick et al. (2011) have shown that particle size, bulk density and pH were the most influential soil properties to resistivity. Pedotransfer functions for hydraulic conductivity and electrical resistivity are based on very similar groups of soil properties. It gives us great opportunities to work out new multivariate pedotransfer functions as a direct connection between electrical resistivity and saturated hydraulic conductivity. It was noticed that there is no direct connection between the resistivity and the saturated hydraulic conductivity. Resistivity is very high (400–700 Ω.m) if dry sand is measured (see Samples no. 11 and 12), but there is no significant connection in any other case (Table 1). The only permanent soil property from the studied ones influencing the resistivity is the grain size (D50). Besides, two other factors have important effects on resistivity, but they are changeable over time: soil moisture and the degree of the soil or sediment compaction. This latter one can be quantified by bulk density and porosity.

CONCLUSION

Based on electrical resistivity tomography results with a precise analysis of grain size and their related physical parameters used for monitoring the compositional materials of two different levee sections along the Tisza and Maros rivers, we conclude that the main components of investigated Tisza levee section are medium and fine silts, however, the situation of the investigated Maros levee section shows more variation of different materials which are fine, medium, and coarse silt, moreover, fine, medium, and coarse sand. The investigated section of the Tisza levee showed low resistivity values, indicating the fine-grained materials' conductivity. In contrast, the investigated section of the Maros levee showed high resistivity values, indicating the resistivity nature of higher grain size sediments forming this section, especially noticed on the protected side of the levee. In general, there is a similarity in the compositional materials and their resistivity range which form the core of the investigated Tisza and Maros levee sections. Regarding the analysis of different physical properties of the two levee systems like resistivity, porosity, density, water content, grain size, and saturated hydraulic conductivity, the compositional materials of the Maros levee could be distinguished well and showed more variation when it is compared to the compositional materials of Tisza levee. It means that the physical properties of levee materials are very important, and they are recommended when carrying out further levee investigations.

We concluded that the samples collected from the Tisza levee show an aquitard nature. In contrast, most of the samples collected from the Maros levee exhibit non-aquitard nature, which illustrates the difference in levee composition in terms of flood risk or flood safety. We also concluded that with the help of the saturated hydraulic conductivity analysis, the cores of the investigated Tisza and Maros levee sections show similarity in the filtration process, which reflects the ability of levees to protect from flooding.

ACKNOWLEDGEMENTS

We acknowledge Szabolcs Gáti for his contribution to ERT measurements. We thank Dávid Filyó and Gergő Magyar for their immense help during drilling. We also thank Istvan Fekete for his assistance in measuring the laboratory samples.

REFERENCES

Abu-Hassanein, Z. S., Benson, C. H., Blotz, L. R. 1996. Electrical resistivity of compacted clays. *Journal of Geotechnical Engineering*, 122(5):397–406. DOI: 10.1061/(ASCE)0733-9410(1996)122:5(397)

Alakukku, L. 1996. Persistence of soil compaction due to high axle load traffic. I. Short-term effects on the properties of clay and organic soils. *European Journal of Soil Science*, 37, 211–222. DOI: 10.1016/0167-1987(96)01017-3

Alexander, J., Wilson, R., Green, W. 2012. A Brief History and Summary of the Effects of River Engineering and Dams on the Mississippi River System and Delta. *Pubsusgsgov, Circular* 1, 53. Online available at: http://pubs.usgs.gov/circ/1375/

Alpaslan, N., Bayram, M. 2020. Landslide study with 2D electrical resistivity tomography (ERT): A case study from Turkey. *Carpathian Journal of Earth and Environmental Sciences*, 15(2), 391–403. DOI: 10.26471/cjees/2020/015/139

Asch, T.H., Deszcz-Pan, M., Burton, B.L., Ball, L.B. 2008. Geophysical characterisation of American River levees, Sacramento, California, using electromagnetics, capacitively coupled resistivity, and dc resistivity. USGS Open File Report (2008-1109, 12 pp). Online available at: https://pubs.usgs.gov/of/2008/1109/index.html

Bakula, K., Salach, A., Wziątek, D.Z., Ostrowski, W., Górski, K., Kurczyński, Z. 2017. Evaluation of the accuracy of lidar data acquired using a UAS for levee monitoring: preliminary results. *Int. J. Remote Sens.*, 38(8–10), 2921–2937. DOI: 10.1080/01431161.2016.1277044

Beck, Y.L., Lopes, S. P., Ferber, V., Côte, P. 2011. Microstructural Interpretation of Water Content and Dry Density Influence on the DC-Electrical Resistivity of a Fine-Grained Soil. *Geotechnical Testing Journal*, 34(6), 694–707. DOI: 10.1520/GTJ103763

Borgatti, L., Forte, E., Mocnik, A., Zambrini, R., Cervia, F., Martinucci, D., Pellegrini, F., Pillon, S., Prizzon, A., Zamariolo, A. 2017. Detection and characterisation of animal burrows within river embankments by means of coupled remote sensing and geophysical techniques: Lessons from River Panaro (northern Italy). *Eng. Geol.*, 226, 277–289. DOI: 10.1016/j.enggeo.2017.06.017

Busato, L., Boaga, J., Peruzzo, L., Himi, M., Cola, S., Bersan, S., Cassiani, G. 2016. Combined geophysical surveys for the characterisation of a reconstructed river embankment. *Eng. Geol*., 211, 74–84. DOI: 10.1016/j.enggeo.2016.06.023

Cardarelli, E., Cercato, M., De Donno, G. 2014. Characterisation of an earth-filled dam through the combined use of electrical resistivity tomography, P- and SH-wave seismic tomography and surface wave data. *J. Appl. Geophys.*, 106, 87–95. DOI: 10.1016/j.jappgeo.2014.04.007

Casagrande A. 1937. Seepage Through Dams. Journal of the New England Water Works Association, republished in Contributions to Soil Mechanics 1925-1940, Boston Society of Civil Engineers, Boston, MA, pp. 295-336. June, 1937. Online available at: https://kupdf.net/download/seepage-through-dams-casagrande-1937_59865910dc0d603d7a300d1d_pdf

Chlaib, H.K., Mahdi, H., Al-Shukri, H., Su, M.M., Catakli, A., Abd, N. 2014. Using ground penetrating radar in levee assessment to detect small-scale animal burrows. *J. Appl. Geophys.*, 103, 121–131. DOI: 10.1016/j.jappgeo.2014.01.011

Cho, I.K., Yeom, J.Y. 2007. Crossline resistivity tomography for the delineation of anomalous seepage pathways in an embankment dam. *Geophysics*, 72(2), G31–G38. doi: 10.1190/1.2435200

Constable, S.C., Parker, R.L. and Constable, C.G. 1987. Occam's inversion: A practical algorithm for generating smooth models from electromagnetic data. *Geophysics*, 52, 289–300. DOI: 10.1190/1.1442303

Crawford, M.M., Bryson, L.S. 2018. Assessment of active landslides using field electrical measurements. *Eng. Geol.*, 233, 146–159. DOI: 10.1016/j.enggeo.2017.11.012

Dane, J.H., Hopmans, J.W. 2002. Water retention and storage. In: Dane, J.H., Topp, G.C. (Eds.), Methods of Soil Analysis, Part 4, SSSA Book Ser. 5. SSSA, Madison, Wisconsin, 671–675.

Datsios, Z. G., Mikropoulos, P. N., Karakousis, I. 2017. Laboratory characterisation and modelling of DC electrical resistivity of sandy soil with variable water resistivity and content. *IEEE Transactions on Dielectrics and Electrical Insulation*, 24(5), 3063–3072. DOI: 10.1109/TDEI.2017.006583

Di Prinzio, M., Bittelli, M., Castellarin, A., Pisa, P.R. 2010. Application of GPR to the moni- toring of river embankments. *J. Appl. Geophys.*, 71(2), 53–61. DOI: 10.1016/j.japgeo.2010.04.002

De Groot-Hedlin, C., Constable, S. 1990. Occam's inversion to generate smooth, two- dimensional models from magnetotelluric data. *Geophysics,* 55, 1613–1624. DOI: 10.1190/1.1649377

Desai C.S. 1970. Seepage in Mississippi River Banks, Analysis of Transient Seepage Using a Viscous-Flow Model and Numerical Methods, Miscellanous Paper S-70-3, Report 1. USACE Waterways Experiment Station, Vicksburg, MS.

Farzamian M., Fernando A. Monteiro Santos, Mohamed A. K. 2015. Application of EM38 and ERT methods in estimation of saturated hydraulic conductivity in unsaturated soil. *Journal of Applied Geophysics*, 112. 175–189. DOI: 10.1016/j.jappgeo.2014.11.016

Fetter, C. W. 2001. Properties of aquifers. Applied hydrogeology, 625p. University of Wisconsin, Oshkosh. Online available at: https://arjzaidi.files.wordpress.com/2015/09/unimasr-com_e7ce669a880a8c4c70b4214641f93a02.pdf

Galli, L. 1976. Az árvízvédelmi földművek állékonyságának vizsgálata. Budapest: Országos Vízügyi Hivatal, Online available at: https://library.hungaricana.hu/hu/view/VizugyiKonyvek_078/?pg=57&layout=s

García-Tomillo, A., de Figueiredo, T., Dafonte, J. D., Almeida, A., Paz-Gonzalez, A. 2018. Effects of machinery trafficking in an agricultural soil assessed by Electrical Resistivity Tomography (ERT). *Open Agric.*, 3, 378–385. DOI: 10.1515/opag-2018-0042

Giao, P. H., Chung, S. G., Kim, D. Y., and Tanaka, H. 2003. Electric imaging and laboratory resistivity testing for geotechnical investigation of Pusan clay deposits. *Journal of Applied Geophysics*, 52(4), 157–175. DOI: 10.1016/S0926-9851(03)00002-8

Gunn, D. A., Chambers, J. E., Uhlemann, S., Wilkinson, P. B., Meldrum, P. I., Dijkstra, T. A., Haslam, E., Kirkham, M., Wragg, J., Holyoake, S., and others 2015. Moisture monitoring in clay embankments using electrical resistivity tomography. *Construction and Building Materials*, 92, 82–94. DOI: 10.1016/j.conbuildmat.2014.06.007

Hadzick, Z. Z., Guber, A. K., Pachepsky, Y. A., Hill, R. L. 2011. Pedotransfer functions in soil electrical resistivity estimation. *Geoderma*, 164. 195–202. DOI: 10.1016/j.geoderma.2011.06.004

Hibert, C., Grandjean, G., Bitri, A., Travelletti, J., Malet, J. P. 2012. Characterising landslides through geophysical data fusion: example of the La Valette landslide (France). *Eng. Geol.*, 128, 23–29. DOI: 10.1016/j.enggeo.2011.05.001

Himi, M., Casado, I., Sendros, A., Lovera, R., Rivero, L., Casas, A. 2018. Assessing preferential seepage and monitoring mortar injection through an earthen dam settled over a gypsiferous substrate using combined geophysical methods. *Engineering Geology*, 246, 212–221. DOI: 10.1016/j.enggeo.2018.10.002

Inazaki, T., Sakamoto, T. 2005. Geotechnical characterisation of levee by integrated geophysical surveying. Proceedings of the International Symposium on Dam Safety and Detection of Hidden Troubles of Dams and Dikes. Online available at: https://citeseerx.ist.psu.edu/document?repid=rep1&type=pdf&doi=7fda76b655ae47c9d132792afa19bb260e0acf56

Jodry, C., Palma Lopes, S., Fargier, Y., Sanchez, M., Côte, P. 2019. 2D-ERT monitoring of soil moisture seasonal behaviour in a river levee: A case study. *Journal of Applied Geophysics*, 167, 140–151. DOI: 10.1016/j.jappgeo.2019.05.008

Jerabek, J., Zumr, D., Dost´al, T. 2017. Identifying the plough pan position on cultivated soils by measurements of electrical resistivity and penetration resistance. *Soil Tillage Res.*, 174, 231–240. DOI: 10.1016/j.still.2017.07.008

Kalinski, R. J., Kelly, W. E., 1993. Estimating water content of soils from electrical resistivity. *Geotechnical Testing Journal*, 16(3), 323–329. DOI: 10.1520/GTJ10053J

Kearey, P., Brooks, M., Hill, I. 2013. An introduction to geophysical exploration. John Wiley & Sons. Department of Earth Sciences University of Bristol 281 Pages.

Keller G.V., Frischknecht F.C. 1966. Electrical methods in geophysical prospecting. Pergamon Press Inc., Oxford. 536 pages. Online avalilable at: https://archive.org/details/electricalmethod00kell/page/n9/mode/2up

Kiss, T., Nagy, J., Fehérvári, I., Amissah, G. J., Fiala, K., Sipos, G. 2021. Increased flood height is driven by local factors on a regulated river with a confined floodplain, Lower Tisza, Hungary. *Geomorphology*, 389, 107858. DOI: 10.1016/j.geomorph.2021.107858

Kiss, T., Fiala, K., Gy, Sipos, Szatmári, G. 2019. Long-term hydrological changes after various river regulation measures: are we responsible for flow extremes. *Hydrol. Res.*, 50(2), 417–430. DOI: 10.2166/nh.2019.095

Knox, R. L., Morrison, R. R., Wohl, E. E. 2022. Identification of artificial levees in the contiguous United States. *Water Resources Research*, 58(4), e2021WR031308. DOI: 10.1029/2021WR031308

Kovács, D. 1979. Árvízvédelem, folyó-és tószabályozás, víziutak Magyarországon (Flood control, regulation of rivers and lakes and waterways in Hungary). National Water Management Authority (OVH), Budapest. 734 pages.

Kun, Á., Katona, O., Sipos, G., Barta, K. 2013. Comparison of pipette and laser diffraction methods in determining the granulometric content of fluvial sediment samples. *Journal of Environmental Geography*, 6(3-4), 49–54. DOI: 10.2478/jengeo-2013-0006

Lászlóffy, W. 1982. The Tisza. Akadémiai Kiadó, Budapest, p. 610 (in Hungarian)

Li Y., Craven J., Schweig E.S., Obermeir S.F. 1996. Sand Boils Induced by the 1993 Mississippi River Flood: Could They One Day be Misinterpreted as Earthquake Induced Liquefaction. *Geology*, 24(2), 171–174. DOI: 10.1130/0091-7613(1996)024<0171:SBIBTM>2.3.CO;2

Loke, M. H. 2004. Tutorial: 2-D and 3-D Electrical Imaging Surveys, 2004 Revised Edition. Tutorial: 2-D and 3-D Electrical Imaging Surveys, July, p. 136. Online available at: https://sites.ualberta.ca/~unsworth/UA-classes/223/loke_course_notes.pdf

Lóczy, D., Kis, É., Schweitzer, F. 2009. Local flood hazards assessed from channel morphometry along the Tisza River in Hungary. *Geomorphology*, 113, 200–209. DOI: 10.1016/j.geomorph.2009.03.013

Morelli, G., Francese, R. 2013. A fast and integrated geophysical imaging system for large-scale levee monitoring. In: Symposium on the Application of Geophysics to Engineering and Environmental Problems, (Denver, Colorado, 17–21 March 2013). DOI: 10.4133/segeep2013-261.1

Nagy L. 2010. Az árvízvédelmi gátak hossza. Nemzetközi összehasonlítás, *Hidrológiai Közlöny*, 90(5), 65–67 (in Hungarian). Online available at: http://www.hidrologia.hu/vandorgyules/34/dolgozatok/word/0216_nagy_laszlo.pdf

Nasta P., Szabó, B., Romano, N. 2021. Evaluation of pedotransfer functions for predicting soil hydraulic properties: A voyage from regional to field scales across Europe. *Journal of Hydrology: Regional Studies*, 37, 20 pp. DOI: 10.1016/j.ejrh.2021.100903

OVF 2014. Árvízi kockázati térképezés és stratégiai kockázatkezelési terv készítése (Flood risk mapping and strategic risk management plan), project report of the National Water Directorate Hungary, Online available at: http://www.vizugy.hu/vizstrategia/documents/B91A47EC-E3B8-4D58-A15F-3E522958BEE8/Orszagos_elontes_1e_web.pdf

Ottoni, M. V., Filho, T. B. O., Lopes-Assad, M. L. R. C., Filho, O. C. R. 2019: Pedotransfer functions for saturated hydraulic conductivity using a database with temperate and tropical climate soils. *Journal of Hydrology*, 575, 1345–1358. DOI: 10.1016/j.jhydrol.2019.05.050

Ojha C. S. P., Singh, V. P., Adrian, D., D. 2001. Influence of Porosity on Piping Models of Levee Failure. *ASCE, Journal of Geotechnical and Geoenvironmental Engineering*, 120(12), 1071–1074. DOI: 10.1061/(ASCE)1090-0241(2001)127:12(1071)

Perri, M.T., Boaga, J., Bersan, S., Cassiani, G., Cola, S., Deiana, R., Simonini, P., Patti, S. 2014. River embankment characterisation: the joint use of geophysical and geotechnical techniques. *J. Appl. Geophys.*, 110, 5–22. DOI: 10.1016/j.jappgeo.2014. 08.012

Pereira, J.O., Defossez, P., Richard, G. 2007. Soil susceptibility to compaction as a function of some properties of a silty soil as affected by tillage system. *European Journal of Soil Science*, 58, 34–44. DOI: 10.1111/j.1365-2389.2006.00798.x

Popescu, M., Șerban, R. D., Urdea, P., Onaca, A. 2016. Conventional geophysical surveys for landslide investigations: Two case studies from Romania. *Carpathian Journal of Earth and Environmental Sciences*, 11(1), 281–292. Online available at: https://www.researchgate.net/profile/Petru-Urdea/publication/290390568_Conventional_geophysical_surveys_for_landslide_investigations_Two_case_studies_from_Romania/links/569a0ccf08ae748dfb019eb4/Conventional-geophysical-surveys-for-landslide-investigations-Two-case-studies-from-Romania.pdf

Reynolds, W. D., Elrick, D. E. 2002. Pressure infiltrometer. In: Dane, J. H., Topp, G. C. (Eds.), Methods of Soil Analysis: Part 4. Physical Methods. Soil Sci. Soc. Am., Inc., Madison, WI, 826–836. DOI: 10.4236/jep.2016.712146

Richard, G., Cousin, I., Sillon, J.F., Bruand, A., Guerif, J. 2001. Effect of compaction on the porosity of a silty soil: influence on unsaturated hydraulic properties. *European Journal of Soil Science*, 52, 49–58. DOI: 10.1046/j.1365-2389.2001.00357.x

Romero-Ruiz, A., Linde, N., Keller, T., Or, D. 2018. A Review of Geophysical Methods for Soil Structure Characterization. *Reviews of Geophysics*, 56(4), 672–697. DOI: 10.1029/2018RG000611

Robain, H., Descloitres, M., Ritz, M., Atangana, Q. Y. 1996. A multiscale electrical survey of a lateritic soil system in the rain forest of Cameroon. *Journal of Applied Geophysics*, 34(4), 237–253. DOI: 10.1016/0926-9851(95)00023-2

Robinson, D. A., Campbell, C. S., Hopmans, J. W., Hornbuckle, B. K., Jones, S. B., Knight, R., Ogden, F., Selker, J., Wendroth, O. 2008. Soil moisture measurement for ecological and hydrological watershed-scale observatories: a review. *Vadose Zone J.*, 7, 358–389. DOI: 10.2136/vzj2007.0143

Samouelian, A., Cousin, I., Tabbagh, A., Bruand, A., Richard, G. 2005. Electrical resistivity survey in soil science: a review. *Soil and Tillage Research*, 83, 173–193. DOI: 10.1016/j.still.2004.10.004

Schwartz, B. F., Schreiber, M. E., Yan, T. 2008. Quantifying field-scale soil moisture using electrical resistivity imaging. *Journal of Hydrology*, 362(3), 234–246. DOI: 10.1016/j.jhydrol.2008.08.027

Schweitzer F. 2002, Pleisztocen. In: Karatson D. (ed.) Pannon Enciklopedia Kertek, Budapest, 130–135.

Sheishah D., Sipos G., Hegyi A., Kozák P., Abdelsamei E., Tóth Cs., Onaca A., Páll, D. G. 2022. Assessing the Structure and Composition of Artificial Levees Along the Lower Tisza River (Hungary). *Geographica Pannonica Journal*, 26(3), 258–272. DOI: 10.5937/gp26-39474

Sjödahl, P., Dahlin, T., Johansson, S. 2009. Embankment dam seepage evaluation from resistivity monitoring data. *NSG*, 7(5–6), 463–474. DOI: 10.3997/1873–0604.2009023

Szűcs P., Nagy L., Ficsor J., Kovács S., Szlávik L., Tóth F., Keve G., Lovas A., Padányi J., Balatonyi L., Baross K., Sziebert J., Ficzere A., Göncz B., Dobó K. 2019 Árvízvédelmi ismeretek (Flood Protection). Online available at: http://hdl.handle.net/20.500.12944/13490 (in Hungarian)

Tabbagh, J., Samouëlian, A., Tabbagh, A., Cousin, I. 2007. Numerical modelling of direct current electrical resistivity for the characterisation of cracks in soils. *Journal of Applied Geophysics*, 62(4), 313–323. DOI: 10.1016/j.jappgeo.2007.01.004

Tímár, G. 2006. Decrease of the flood conveying capacity of the Middle Tisza River, Hungary, due to the regional surface deformation. *EGU, Geophysical Research Abstracts*, 8, 5701. DOI: 10.13140/2.1.4415.8401

Tóth, B., Weynants, M., Nemes, A., Makó, A., Bilas, G., Tóth, G. 2015. New generation of hydraulic pedotransfer functions for Europe. *European Journal of Soil Science*, 66. 226–238. DOI: 10.1111/ejss.12192

USACE – U.S. Army Corps of Engineers 2000. EM 1110-2-1913, Engineering and Design - Design and Construction of Levees. Department of the Army, USACE, Washington, DC. Online available at: https://www.yumpu.com/en/document/view/346990/department-of-the-army-em-1110-2-1913-us-army-corps-of-

Waxman, M. H., Smits, L. J. M. 1968. Electrical conductivities in oil-bearing shaly sands. *Society of Petroleum Engineers Journal*, 8(02), 107–122. DOI: 10.2118/1863-A

Zhu, J.J., Kang, H.Z., Gonda, Y. 2007. Application of Wenner configuration to estimate soil water content in pine plantations on sandy land. *Pedosphere*, 17, 801–812. DOI: 10.1016/S1002-0160(07)60096-4